Hop Count Analysis for Greedy Geographic Routing

Quanjun Chen , Salil S. Kanhere , Mahbub Hassan
School of Computer Science and Engineering,
The University of New South Wales, Sydney, Australia,
Email: {quanc, salilk, mahbub}@cse.unsw.edu.au

UNSW-CSE-TR-0824

December 2008

Abstract

Hop count is a fundamental metric in multi-hop wireless ad-hoc network. It has a determinative effect on the performances of wireless network, such as throughput, end-to-end delay and energy consumption. Identifying hop count metric, including the distribution function and the mean value, is therefore vital for analyzing wireless network performance. This paper proposes a theoretical model to accurately analyze the hop count distribution and its mean value. Given a communication pair, its hop count metric is dependent on the routing protocol selected and the network topology determined by the physical radio model. At routing layer, our model focuses on the widely used greedy routing. At physical layer, the model investigate the ideal radio model, and a more realistic radio model, e.g. log-normal shadowing model. We conduct a rich set of simulation to validate our analytical model. The comparison results show that the simulation results closely match with the analysis results. The analytical model is further validated through a trace driven simulation of a practical vehicular ad-hoc network that exhibits realistic topologies of public transport buses in a metropolitan city.

I. Introduction

Multi-hop communications have been popular adopted in wireless ad-hoc networks. It extends the connectivity of nodes from local area to a large scale network. Multi-hop communications also bring some challenges to the network. For example, the wireless transmission of each hop consumes scarce resources such as bandwidth and energy. It also introduces the chance of packet lost and extra delay. The hop count, measured as the number of transmissions that a packet experiences from a source to a destination, becomes a fundamental metric in wireless network performance [1-6].

Despite its importance, hop count has not been fully investigated in the literature. Most previous work [1-3] uses a naive and unrealistic approach to estimate of hop count. Their estimations simplify hop count as the ratio of source-to-destination Euclidean distance to radio range. Several work [7-13] have aimed to analyze hop count metric to give a more accurate result. However, most of these work used an assumption of the ideal radio model, where radio coverage is a perfect disk and no random fading presents. This radio model is far from realistic [14] and therefore limits the application of their results.

In this paper, we aim to accurately analyze the hop count distribution and the mean value given a communication pair in random wireless ad-hoc networks. Intuitively the hop count between a source and a destination depends on the routing path being selected. The routing fundamental considered in our model is *greedy gregraphic routing*, a well known concept considered by many routing protocols [15], [16], [17]. The underlying principle used in these protocols involves selecting the next routing hop from amongst a node's neighbors, which is geographically closest to the destination. Since the forwarding decision is based entirely on local knowledge, it obviates the need to create and maintain routes for each destination. By virtue of these characteristics, geographic routing protocols are highly scalable and particularly robust to frequent changes in the network topology. Furthermore, since the forwarding decision is made *on the fly*, each node always selects the optimal next hop based on the most current topology. Several studies [15], [18], [19] have shown that these routing protocols offer significant performance improvements over topology-based routing protocols such as DSR [20] and AODV [21].

For developing an analytical model of the hop count it is necessary to use an appropriate model that abstracts the wireless communication characteristics of a realistic environment. In our analysis we have used both the idealistic radio model and the realistic log-normal shadowing model, thus enabling us to compare the impact of the two on the results. To the best of our knowledge, this work is the first attempt at developing a comprehensive model for characterizing the hop count for greedy geographic routing.

Since the hop count is closely determined by the behavior of packets' progress toward the destination,

i.e. how the packet is forwarded towards the destination, we use a discrete Markov chain to model the hop-by-hop progress of a packet from the source to the destination. We firstly identify the state transition probability in this Markov china model. Then, based on the state transition probability, we recursively calculate the hop count distribution and the mean value. We conduct a rich set of simulations to validate our analytical model. The comparison results well justify our proposed model. The analysis results are also confirmed through a trace driven simulation of a practical vehicular ad-hoc network that exhibits realistic topologies of public transport buses in a metropolitan city.

The main contributions of this paper are as follows: 1)We accurately analyze the hop count distribution and mean value for greedy routing in both ideal radio and realistic radio environments (i.e. log-normal shadowing radio). 2) Our analysis results show that the widely used hop count estimation, i.e. the ratio of source-to-destination Euclidean distance to radio range, under-estimates the hop count in ideal radio model, while may over-estimate the hop count in realistic radio model. 3) We demonstrate that the well accepted concept, i.e. the greedy routing can approximately find the shortest path in a dense network, only works for ideal radio model but cannot apply to realistic radio model.

The rest of the paper is organized as follows. In Section II, we discuss the related work. Section III presents the overview of the analytical model. In Section IV, we analyze the state transition probability of the Markov chain that models hop-by-hop progress of a packet in greedy routing. We then formulate the hop count distribution and the mean hop count in Section V. Section VI presents extensive simulations to validate our theoretical results. Finally, we give conclusions in the last Section VII.

II. Related Work

The most-widely used estimation of hop count employs a naive and unrealistic estimation [1, 2]. This simple estimation assumes that the intermediate node can always find the next hop at the border of radio range and the next hop lies on the straight line connecting the source and the destination. Thus the hop count is simplified as the source-to-destination Euclidean distance divided by the radio range. This assumption is far from accurate since forwarding nodes often cannot find a neighbor at the border of its radio coverage.

Many work have been proposed to analyze the hop count metric with an assumption of an ideal radio model where no random fading presents, e.g. [7-12]. Kleinrock and Silvester [7] presented an approach to approximately estimate the mean hop count occurred in Most Forward with in Radius (MFR) routing protocol.They firstly formula the average progress per hop, i.e. the average distance that each

hop can progress towards to the destination. Then the hop count is estimated as the ratio of the source-to-destination distance to the average progress per hop.

Lebedev and Steyaert [8] tried to analyze the mean hop count in flood-based routing. They assumed that the radio coverage is a square shape, which is split into four quadrants, and the forwarding node only select the next hop from one of the four quadrants that orients to the destination. Swades De [9], [22] proposed a sound analytical model to estimate the mean hop count incurred in greedy routing. Similar to [7], they formulated the average progress per hop, then used this result to estimate average hop count given a source-to-destination distance. They also illustrate the hop count distribution by numerical simulation.

Zhao and Liang [10] generalized a formula to estimate the hop count based on statistic results of simulation. Bettstetter and Eberspaecher [11] derived the probability that two randomly selected nodes is one-hop connected or two-hop connected. For a larger hop count, they assumed that nodes density is infinite and presented a lower bound formula. Dulman et. al. [12] formulated the hop count distribution of the shortest path routing in one dimension network and gave an approximate analysis on two dimension network case.

All the above mentioned previous work have an assumption of ideal radio model. Mukherjee and Avidor [13] studied the hop count distribution in a more realistic model, i.e. log-normal shadowing radio model, with a focus of shortest path routing. Given the computation complexity of their formula, it takes tremendous time to compute the hop count distribution and the mean hop count as well. Because of this, they [13] only present the analysis results for the probability of one-hop and two-hop connection. For a larger hop count, they presented some simulation results.

To the best of our knowledge, we believe that this work is the first of its kind to study the hop count distribution for greedy routing that considerate a realistic radio model.

III. Overview of the System Model

For mathematical tractability, we make the following simplifying assumptions:

- The node distribution follows a homogenous Poisson point process with a density of ρ sensors per unit area, which can approximate uniform distribution for large area. This assumption has been widely used in analyzing multi-hop wireless ad-hoc networks [23], [24], [25].
- No Boundary: In a typical ad hoc deployment, nodes located near the network boundary have fewer neighbors that nodes located elsewhere. To avoid this distinction, we ignore the existence of the

boundary. Consequently, the probability distribution function for the number of neighbors at each node is identical [26].

- All nodes have identical transceivers and the wireless links are assumed to be symmetric.
- Complete Knowledge of Local Topology: We assume that nodes always have an up-to-date view of their local topology, i.e. each node is aware of the locations of its immediate neighbors. The nodes can employ a neighbor discovery protocol for this purpose. Consequently, each intermediate node can always find the optimal next hop.
- The network is dense enough such that the greedy routing always succeeds in finding a next hop node that advances the data packet towards the sink. In other words, we assume that the forwarding strategy does not encounter a *local minima condition* and thus, neglect the effect of planar routing, which is employed in these circumstances.

The above assumptions, some of which are somewhat unrealistic, are necessary in making the analysis tractable. However, in our simulation study, we relax several of these assumptions (e.g: uniform distribution of the nodes) to create more realistic scenarios and compare the resulting outcomes to those from our analysis.

In the first part of our analysis we consider an ideal radio model, wherein the signal attenuation between any two nodes is a function of the Euclidean distance separating the nodes. Consequently, in this idealistic environment, the radio coverage of a sensor node is a perfect circular disc with the radius equal to its radio range. However, in reality, the signal attenuation is not solely dependent on the distance. For example, signal reflection or signal noise can also attenuate the signal. To make our analytical results more realistic, we extend our analysis and incorporate the log-normal shadowing radio model. This model adds a random signal loss component to the purely distance-dependent signal attenuation. As will be elaborated later, we have observed significant differences in the analytical results with the two models. Note that, by employing these two radio models, we implicitly assume that signal attenuation over different link are independent. For the sake of mathematical tractability, we do not consider signal correlation among different links. This link independent log-normal shadowing model has been widely used to approximate the real environment [14, 15, 16].

Assuming that the distance between the source and destination is known, our analysis seeks to develop a model for analyzing the hop count from the source to the destination incurred in greedy routing. We use a discrete Markov chain to model the hop-by-hop progress of a packet from the source to the destination. The state of the Markov chain is defined as the Euclidean distance (measured in some consistent metric unit, e.g. meters) between the current forwarding node that holds the packet and the destination. Ideally,

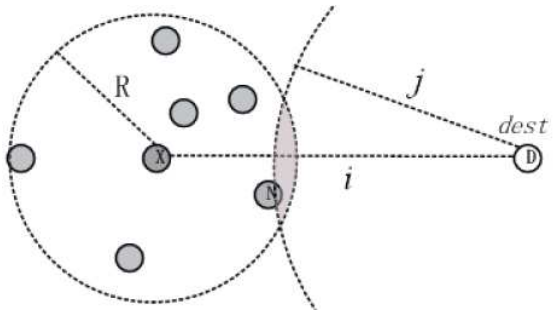

Fig. 1. Example of state transition (from state i to state j)

this distance should be modeled as a continuous random variable. However, to simplify our model, we use a discrete state space to approximately represent the continuous distance values. We quantize the distances resulting in a state space of $(0, \varepsilon, 2\varepsilon, ..., n\varepsilon, ...)$, where the parameter ε is the interval of the state space (i.e. the quantization coefficient). When the interval ε is small enough, the discrete state space approximates the original continuous distance metric.

We elaborate on the state transition of the Markov chain using the example illustrated in Fig. 1, Assume that a packet is currently held by node X as it makes its way towards the destination, node D. Since node X is at a distance i from the destination, the current state for this packet is i. Assume that the next hop node chosen by node X using greedy forwarding is node N, which is at a distance of j from the destination. The packet forwarding operation thus results in a state transition from i to j for the packet. In general, the hop-by-hop progress made by a packet towards the destination can be represented by a series of states that the packet transitions through, eventually culminating in state 0 when the packet reaches the destination.

Our analysis is composed of the following steps. The first step involves determining the state transition probabilities for the Markov chain (section IV-A) using geometric calculation assuming the ideal circular disc radio model. Next we extend this to include the log-normal shadowing model (section IV-B). Based on the transition probabilities, we recursively compute the hop count distribution and the mean value given a communication pair (section V). The main symbols used in the paper are listed in Table I.

IV. Analytical Model of the State Transition Probability

We first evaluate the state transition probabilities assuming the ideal circular disc radio model. Next we extend this to include the log-normal shadowing model.

TABLE I

LIST OF MAIN SYMBOLS USED IN THE ANALYSIS

Symbol	Definition
R	Average radio range of sensors
ρ	Node density, i.e. the number of nodes per unit area
ε	Quantization interval
i, j, d	Euclidean distance from a sensor to the destination
ξ	Signal randomness parameter in log-normal shadowing radio model
$P_{\wedge}(s)$	The probability that two nodes separated by distance s can communicate with each other
$P_{i,j}$	State transition probability. i.e. the probability that a sensor at distance i from the sink can forward its packets to the sensor at distance j

A. Evaluating the State Transition Probability for the Ideal Radio Model

For the ideal radio model, a node can only communicate with other nodes that are located within the circular coverage region of this node. Let R be the radio range of each nodes. For two nodes separated by a distance s, the probability that they have a direct link, denoted as $P_{\wedge}(s)$, is

$$P_{\wedge}(s) = \begin{cases} 1 & \text{if } i \leq R, \\ 0 & \text{if } i > R. \end{cases} \tag{1}$$

We employ an approach that uses geometric computations and probability theory to prove the following,

Theorem 1: In the context of an ideal radio model, the transition probability of a packet from state i to j when employing greedy routing is,

$$P_{i,j} = \begin{cases} 1 & \text{if } i \leq R \text{ and } j = 0, \\ \exp(-\rho A_{i,j}) - \exp(-\rho A_{i,j+\varepsilon}) & \text{if } i > R \text{ and } i - R \leq j < i, \\ 0 & \text{others,} \end{cases} \tag{2}$$

where $A_{i,j}$ is,

$$A_{i,j} = R^2 \arccos \tfrac{i^2+R^2-j^2}{2iR} + j^2 \arccos \tfrac{i^2+j^2-R^2}{2ij} - \tfrac{\sqrt{(R+i+j)(R+i-j)(R-i+j)(i+j-R)}}{2} \tag{3}$$

Proof:

Assume that a packet is currently at node X as it makes its way towards the destination. Let node X be at a distance i from the destination as illustrated in Fig. 2. Consequently the packet is currently

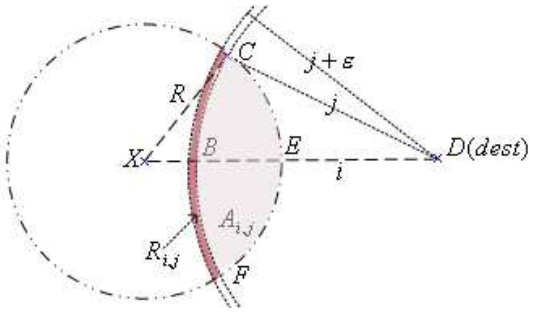

Fig. 2. Illustration used to prove Theorem 1.1

in state i. The probability that the packet is forwarded to a sensor at distance j and thus resulting in a transition to state j is the probability that node X finds a neighbor at distance j as the next hop.

We start with a simple case, where $i \leq R$, i.e. the destination node is within radio coverage of the current node X. Hence, as the next hop is the destination, the state i must transition to state 0. Consequently, we have,

$$P_{i,j} = \begin{cases} 1 & \text{if } i \leq R \text{ and } j = 0, \\ 0 & \text{if } i \leq R \text{ and } j > 0. \end{cases} \tag{4}$$

Now let us consider the situation where $i > R$. Recall that, we have assumed that greedy routing can always succeed in finding a next hop node which is closer to the destination. Thus the next hop of node X must has a distance that is less than i from the destination. In other words, the probability that the next hop node lies outside distance region $[i - R, i)$, is zero. Therefore, we have,

$$P_{i,j} = 0, \qquad \text{if } i > R \text{ and } (j < i - R \text{ or } j \geq i) \tag{5}$$

Now, we discuss the more complicated and plausible case where, $i - R \leq j < i$. In greedy routing, if the next hop of node X is at distance j, it implies that at least one neighbor of node X is at distance j and none of its other neighbors are closer to the destination than j. Thus the transition probability is the probability that at least one neighbor of node X lies on the perimeter of the curve of radius j centered at the destination (see Fig. 2) with no neighbors located to the right of this curve. Since we assume a discrete state space with ε as the interval of the state space, we can approximate the curve as a ring of thickness ε, as illustrated in Fig. 2. Let $R_{i,j}$ represent the region of this thin ring that intersects with the radio range of node X (narrow dark region in Fig. 2). We also denote $A_{i,j}$ as the area of the light shaded region in Fig. 2, which is the intersecting region between the radio coverage of node X and a

circle of radius j centered at the destination. $R_{i,j}$ and $A_{i,j}$ are also used to represent the area of each region referred.

Now, the transition probability $P_{i,j}$ is the probability that at least one node lies inside region $R_{i,j}$ and the no nodes are within $A_{i,j}$. Let P_1 be the probability that at least one node is within $R_{i,j}$, and P_2 be the probability that no nodes lie within $A_{i,j}$.

Recall that, we have assumed that the node distribution follows a homogenous Poisson point process with density ρ. As a property of this assumption, the number of nodes in any region of area A follows a Poisson distribution with mean of ρA. Thus the number of nodes in region $R_{i,j}$ follows a Poisson distribution with mean $\rho R_{i,j}$, and the number of nodes in region $A_{i,j}$ has a Poisson distribution with mean of $\rho A_{i,j}$. Note that, the area of $R_{i,j}$ can be computed as $A_{i,j+\varepsilon} - A_{i,j}$. Consequently, we have,

$$P_1 = 1 - \text{Prob(no node in } R_{i,j}) = 1 - \exp(-\rho R_{i,j}) = 1 - \exp(\rho A_{i,j} - \rho A_{i,j+\varepsilon}) \tag{6}$$

$$P_2 = \text{Prob(no node in } A_{i,j}) = \exp(-\rho A_{i,j}) \tag{7}$$

In the Poisson point process, the distribution of the number of nodes in any two disjoint region is independent. Thus P_1 and P_2 are independent and we have,

$$P_{i,j} = P_1 \cdot P_2 = \exp(-\rho A_{i,j}) - \exp(-\rho A_{i,j+\varepsilon}) \tag{8}$$

Now we come to compute the area of $A_{i,j}$. As shown in Fig. 2, the area $A_{i,j}$ can be computed as,

$$A_{i,j} = 2(A_{\widehat{CXE}} + A_{\widehat{CDB}} - A_{CXD}) \tag{9}$$

where $A_{\widehat{CXE}}$ is the area of the sector CXE; A_{CXD} is the area of triangle CXD and $A_{\widehat{CDB}}$ is the area of sector CDB. By applying the law of cosines and Heron's formula, we have,

$$\begin{cases} A_{\widehat{CXE}} = \frac{R^2}{2}\angle CXD = \frac{R^2}{2}\arccos\frac{i^2+R^2-j^2}{2iR} \\ A_{\widehat{CDB}} = \frac{R^2}{2}\angle CDX = \frac{j^2}{2}\arccos\frac{i^2+j^2-R^2}{2iR} \\ A_{CXD} = \frac{\sqrt{(R+i+j)(R+i-j)(R-i+j)(i+j-R)}}{4} \end{cases} \tag{10}$$

Combining Equations (9) and (10), we obtain Equation (3). Finally, combining Equations (4), (5), (8) and (3), the theorem is proved. ♠

B. Evaluating the State Transition Probability for the Log-normal Shadowing Radio Model

Next, we study a more realistic radio model. In the log-normal shadowing radio model, the signal attenuation between two nodes is dependent not only on the distance separating the two nodes, but also

a random signal loss. More formally, given a distance s that separates two nodes, the signal attenuation (in dB) from one node to another one is,

$$\beta(s) = \alpha \log_{10}(\frac{s}{\text{reference distance}}) + \beta_1 \tag{11}$$

where α is a path loss rate, and β_1 is a random variable that follows a normal distribution with zero mean and a standard deviation of σ,

$$f(\beta_1) = \frac{1}{\sqrt{2\pi}\sigma} \exp(-\frac{\beta_1^2}{2\sigma^2}) \tag{12}$$

Now two nodes are one-hop neighbors, i.e. they have a direct link between them, only if the signal attenuation between them is less than or equal to a predefined attenuation threshold β_{th}. Thus, for two nodes separated by a distance s, the probability that they have a direct link, denoted as $P_\wedge(s)$, is given by,

$$P_\wedge(s) = Prob(\beta(s) < \beta_{th}) \tag{13}$$

The above equation has been solved by Bettstetter in [23] and the result can be represented by,

$$P_\wedge(s) = \frac{1}{2}\left[1 - erf(\frac{10}{\sqrt{2}\xi} log_{10}\frac{s}{R})\right], \quad \xi = \sigma/\alpha \tag{14}$$

where $R = 10^{\frac{\beta_{th}}{\alpha \cdot 10}}$, is referred to as the *average radio range*, which is the maximum distance that permits the existence of a link between two nodes in the absence of signal randomness. The function $erf(.)$ is defined as follows,

$$erf(z) = \frac{2}{\sqrt{\pi}} \int_0^z \exp(-x^2) dx \tag{15}$$

As an illustrative example, Fig. 3 plots the link probability for the log-normal shadowing model for $R = 50m$ and different values of the random parameter ξ. Note that, the curve has a longer tail for increasing values of ξ, which implies that a node's radio may cover a larger area for larger ξ. Based on the aforementioned characteristics of the log-normal model, we can have the following theorem,

Theorem 2: In the context of the log-normal shadowing radio model, the transition probability of a packet state i to j when employing greedy routing is,

$$P_{i,j} = \begin{cases} P_\wedge(i) & \text{if } j = 0 \text{ and } i > 0, \\ 0 & \text{if } j > 0 \text{ and } j \geq i, \\ [1 - P_\wedge(i)] \cdot \exp(-\pi\rho j^2 P_\wedge(A_{i,j})) \cdot & \\ \quad [1 - \exp(-\pi\rho\varepsilon(2j+\varepsilon)\frac{(j+\varepsilon)^2 P_\wedge(A_{i,j+\varepsilon}) - j^2 P_\wedge(A_{i,j})}{(2j+\varepsilon)\varepsilon})] & \text{others,} \end{cases} \tag{16}$$

Where $P_\wedge(i)$ is defined in equation (43), and

$$P_\wedge(A_{i,j}) = \int_{i-j}^{i+j} P_\wedge(s) f_{i,j}(s) ds \tag{17}$$

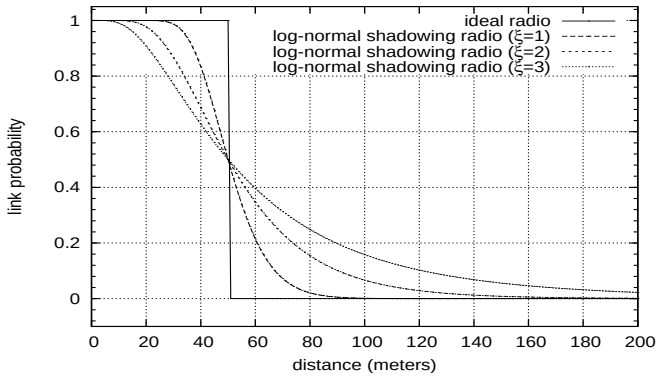

Fig. 3. Link probability with different radio models ($R = 50$)

$$f_{i,j}(s) = \frac{1}{\pi j^2}(j^2\theta^{'} + 2s\phi - i\sin(\phi) + \frac{s^2 + j^2 - i^2}{2}\phi^{'}) \tag{18}$$

$$\begin{aligned} \theta' &= \frac{2s}{\sqrt{4i^2j^2-(i^2+j^2-s^2)^2}} \qquad \phi = \arccos(\tfrac{s^2+i^2-j^2}{2is}) \\ \phi^{'} &= \frac{is}{i\sqrt{4i^2s^2-(s^2+i^2-j^2)^2}}(\tfrac{i^2-j^2}{s^2} - 1) \end{aligned} \tag{19}$$

proof:

We start with the simple case when $j = 0$ and $i > 0$. Assume that a packet is currently in state i, while located at a certain node X. The transition probability of the packet from state i to zero is the probability that there is a direct link between node X and the destination. Thus we have $P_{i,j} = P_{\wedge}(i)$ when $j = 0$ and $i > 0$.

Now let us consider the situation where $j > 0$ and $j \geq i$. Since the next hop of node X must has a distance that is less than i from the destination, the probability that the next hop node lies outside distance region $[0, i)$, is zero. Therefore, we have $P_{i,j} = 0$, when $j > 0$ and $j \geq i$.

In other cases where the next state $j > 0$ and $j < i$, the transition probability $P_{i,j}$ is the multiplication of the following three independent probabilities,

- The probability that no direct link exists between node X and the destination (otherwise the packet can be forwarded to the destination directly), which is $1 - P_{\wedge}(i)$.
- the probability that the node X can find at least one neighbor at distance j, denoted as $1 - P_1$, where P_1 is the probability that there is no neighbor at distance j.
- The probability that no neighbor is within the region that is closer to the destination than j, which is denoted as P_2.

Thus, we have,

$$P_{i,j} = [1 - P_{\wedge}(i)](1 - P_1)P_2, \quad \text{if } j > 0 \text{ and } j < i \tag{20}$$

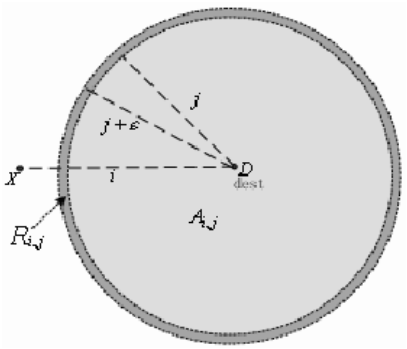

Fig. 4. Illustration used to prove Theorem 1.2

Similar to the previous sub-section, we use a ring of thickness ε to represent the curve that is located at distance j from the destination, as illustrated in Fig. 4. Let $R_{i,j}$ denote the ring area that has distance j to the destination, and Let $A_{i,j}$ represent the shaded disc shaped region that is closer to the destination than j but does not include the location of the destination itself. Note that, the area included under $R_{i,j}$ and $A_{i,j}$ with the log-normal model is much larger as compared with the ideal radio model in section IV-A. The reason being that with the realistic log-normal model the one-hop neighbors of X can located anywhere in the network. On the contrary, in the case of the ideal radio model, the one-hop neighbors are restricted in the circular coverage area of node X. Thus, P_1 is the probability that no direct link exists between X and any node in region $R_{i,j}$, and P_2 is the probability that no direct link exists between X and any node in region $A_{i,j}$.

We first calculate P_1. Since the number of nodes within $R_{i,j}$ is a random variable, according to the law of total probability, we have,

$$P_1 = \sum_{k=0}^{\infty} \Big\{ Prob(\text{k nodes in } R_{i,j}) \cdot \ Prob(\text{no direct link from X to any one of those k nodes}) \Big\} \tag{21}$$

According to the Poisson point process, the number of nodes within $R_{i,j}$ has a Poisson distribution with mean $\rho R_{i,j}$. Also, given that there are k nodes in area $R_{i,j}$, these k nodes are independently distributed [27] [28]. Therefore the existence of a direct link between node X and every node in area $R_{i,j}$ is independent of each other. Let $P_\wedge(R_{i,j})$ be the probability that there exists a direct link between node X and a node within area $R_{i,j}$. Equation (21) can be rewritten as,

$$P_1 = \sum_{k=0}^{\infty} \frac{(\rho R_{i,j})^k}{k!} \exp(-\rho R_{i,j})(1 - P_\wedge(R_{i,j}))^k = \exp(-\rho R_{i,j} P_\wedge(R_{i,j})) = \exp(-\pi\rho\varepsilon(2j+\varepsilon)P_\wedge(R_{i,j})) \tag{22}$$

Similar, for P_2, we can have,

$$P_2 = \exp(-\rho A_{i,j} P_\wedge(A_{i,j})) = \exp(-\pi\rho j^2 P_\wedge(A_{i,j})) \tag{23}$$

Combining Equations (20) (22) and (23), we have,

$$P_{i,j} = \big[1 - P_\wedge(i)\big] \cdot \exp\big[-\pi\rho\varepsilon(2j+\varepsilon)P_\wedge(R_{i,j})\big] \cdot \exp\big[-\pi\rho j^2 P_\wedge(A_{i,j})\big] \tag{24}$$

Next we compute $P_\wedge(R_{i,j})$ and $P_\wedge(A_{i,j})$. According to the definition of $A_{i,j}$, the combined region of $R_{i,j}$ and $A_{i,j}$ can be represented by $A_{i,j+\varepsilon}$. Therefore $P_\wedge(R_{i,j})$ can be represented by $A_{i,j}$ and $A_{i,j+\varepsilon}$. In the Poisson point process distribution, given that a node is present within $A_{i,j+\varepsilon}$, the node is uniformly distributed in the region and it is either inside region $R_{i,j}$ or $A_{i,j}$. By the law of total probability, we have,

$$\begin{aligned} P_\wedge(A_{i,j+\varepsilon}) &= P_\wedge(R_{i,j})Prob(\text{the node is within } R_{i,j}) + P_\wedge(A_{i,j})Prob(\text{the node is within } A_{i,j}) \\ &= P_\wedge(R_{i,j})\frac{(2j+\varepsilon)\varepsilon}{(j+\varepsilon)^2} + P_\wedge(A_{i,j})\frac{j^2}{(j+\varepsilon)^2} \end{aligned} \tag{25}$$

Equivalently, we have,

$$P_\wedge(R_{i,j}) = \frac{(j+\varepsilon)^2 P_\wedge(A_{i,j+\varepsilon}) - j^2 P_\wedge(A_{i,j})}{(2j+\varepsilon)\varepsilon} \tag{26}$$

Combining Equations (24) and (26), we have,

$$P_{i,j} = [1 - P_\wedge(i)] \cdot \exp(-\pi\rho j^2 P_\wedge(A_{i,j})) \cdot [1 - \exp(-\pi\rho\varepsilon(2j+\varepsilon)\tfrac{(j+\varepsilon)^2 P_\wedge(A_{i,j+\varepsilon}) - j^2 P_\wedge(A_{i,j})}{(2j+\varepsilon)\varepsilon})] \tag{27}$$

Finally, we compute the last unknown variable $P_\wedge(A_{i,j})$, i.e., given there exists a node within region $A_{i,j}$, the probability that this node has a direct link with node X. Let $f_{i,j}(s)$ represent the probability that this node is located at distance s from the node X. Based on the law of total probability, we have,

$$P_\wedge(A_{i,j}) = \int_{i-j}^{i+j} P_\wedge(s) f_{i,j}(s) ds \tag{28}$$

Given a node is within region $A_{i,j}$, the distance from this node to node X varies from $(i-j)$ to $(i+j)$. Thus the integral in Equation (28) represents the conditional probability. Following rigorous geometric calculations, $f_{i,j}(s)$ is computed as indicated in Equation (18). The detailed derivation is omitted here due to the limited space.

Finally, combining Equations (27), (28) and (18), the theorem is proved. ♠

We now provide an example to illustrate the state transition probability, $P_{i,j}$. In this example, we assume the following set of parameters, $R = 50m, \varepsilon = 1m, \rho = 0.0019$, the current state of a packet is $i = 100$ and the next state varies from 100 to 0. Fig. 5 illustrates the distribution of the transition probability from state i to the next state j for both radio models under consideration. Note that, the log-normal model reduces to the ideal circular coverage model when the random parameter ξ is equal to zero. For the ideal radio model the peak of the distribution is around $j = 57$ and it reduces to zero for all states beyond 50. This is because of the circular coverage assumption (recall that $R = 50m$). With

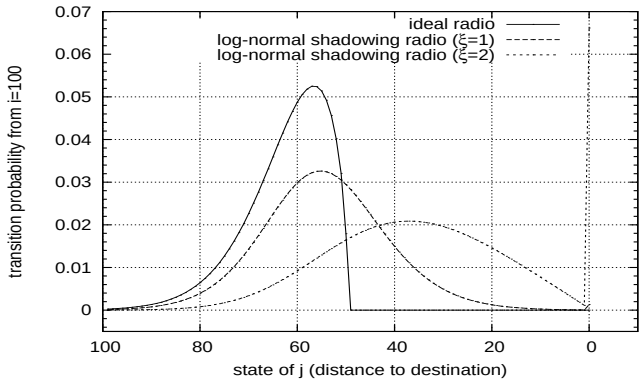

Fig. 5. State transition probability from $i = 100$ ($R = 50$)

the more realistic log-normal model the distribution is more spread out over the entire range and the peak shifts towards the right, i.e., closer to the destination. This effect is more pronounced as the random parameter ξ increases. This is because higher the randomness in the signal, the greater is the chance that a node closer to the destination is chosen as the next hop.

V. Hop Count Distribution and the Mean value

Based on the state transition probability $P_{i,j}$, we now proceed to derive the hop count distribution and the mean value of a communication pair. We also propose some approximations to simplify the mean hop count calculations in this section.

A. Hop Count Distribution

The analysis is independent of the radio model under consideration. One simply has to substitute the appropriate state transition probability equations as derived in the previous section for the radio model under consideration.

Recall that, the state variable in our Markov model represents the distance between the current node and the destination. Based on the transition probability computed in previous sections and using the approach of recursive computation, we obtain the probability distribution function of the hop count as follows,

Theorem 3: Given a source and destination separated by distance i, the probability distribution of hop

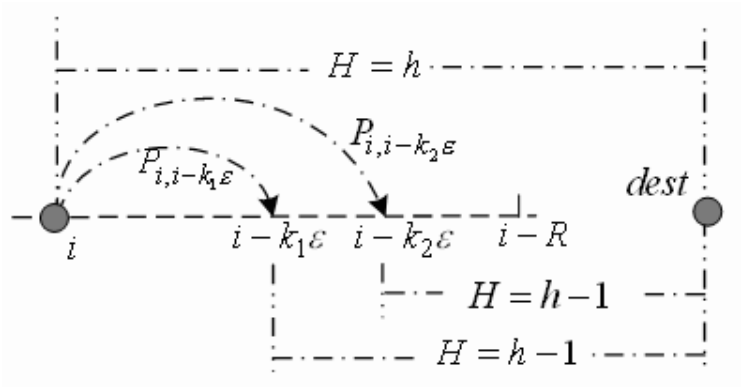

Fig. 6. Computation of the hop count probability distribution

count (denoted as H) in greedy routing is given by,

$$P(H=h|D=i)= \begin{cases} P_{\wedge}(i) & \text{if } h=1, \\ \sum\limits_{j\in(i,0)} P(H=h-1|D=j)P_{i,j} & \text{if } h>1, \end{cases} \tag{29}$$

where $P_{\wedge}(i)$ and $P_{i,j}$ denote the link probability and the state transition probability for the radio model under consideration. For ideal radio model, $P_{\wedge}(i)$ and $P_{i,j}$ are derived in Equation (1) and Theroem 1. For log-normal shadowing radio model, $P_{\wedge}(i)$ and $P_{i,j}$ are derived in Equation (43) and Theroem 2.

Proof:

When $h=1$, the probability that the source is one hop away from the destination is the probability that they have a direct link. Thus,

$$P(H=h|D=i)=P_{\wedge}(i), \qquad \text{if } h=1 \tag{30}$$

For the other cases, we can apply the recurrence computation. As illustrated in Fig. 6, the possible next hop states j originating at i are constrained between i and 0, and each subsequent step in the state space is separated by ε. If the hop count from the current state i to the destination is h, the hop count from the next state j to the destination must be $h-1$. By applying the law of total probability, we have,

$$P(H=h|D=i)=\sum_{j\in(i,0)} P(H=h-1|D=j)P_{i,j} \tag{31}$$

Combining Eqs. (30) and (31), the theorem is proved. ♠

Using Eq. (30), one can readily determine the probability of one hop. Subsequently, using Eq. (31) and the probability of one hop, the probability of two hops can be computed. Similarly, employing recursive computations, the probability of all h hops can be computed.

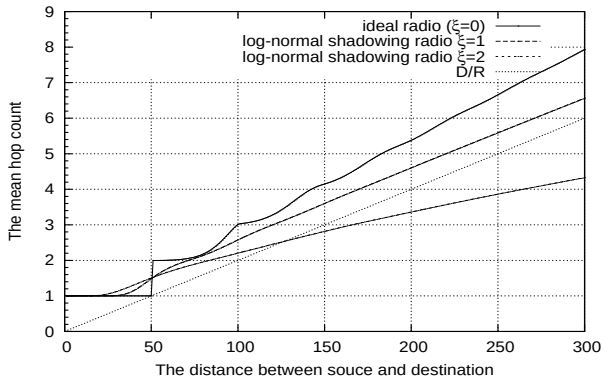

Fig. 7. mean hop count with varying distance and radio model

B. Mean Hop Count

Based on the hop count distribution result of Theorem 3, we can easily calculate the mean hop count for a pair of communication nodes that are separated by distance i. Let $\overline{H(i)}$ represent the mean hop count given i. $\overline{H(i)}$ can be computed as follows,

$$\overline{H(i)} = \sum_{h=1}^{\infty} h \cdot P(H = h | s = i) \tag{32}$$

Now we illustrate the mean hop count for Cons $R = 50m, \varepsilon = 1m, \rho = 0.0019$, the same parameters as used in Fig. 5. Fig. 7 plots the mean hop count as a function of the distance between the source and destination for different radio models. One can readily observe from Fig. 7 that the mean hop count is approximately a linear function of the distance. This observation implies that the ratio of the source-destination distance to the mean hop count is approximately constant. In addition, the slope of the linear line is decreasing when the ξ is increasing. Therefore, given a same source-to-destination distance, a packet in a network with bigger ξ takes less number of hops to reach the destination. Fig. 7 also compare the analysis results with the widely used estimation, i.e. the ratio of source-to-destination Euclidean distance to the radio range. It shows that the widely used estimation under-estimates the mean hop count in ideal radio model, while may over-estimate the mean hop count in realistic radio model when a large random fading presents.

Note that, the above computation of the mean hop count requires us to recursively compute the hop count distribution of the hop count in entire distance space. This computation has a time complexity of $O(i^3)$. It is evident that evaluating the mean hop count for a sizable network can be an considerably computationally intensive task. Hence, in the next subsection, we evaluate an $O(1)$ technique for estimating the mean hop count. We also demonstrate that our estimate is quite accurate, especially when $L >> R$.

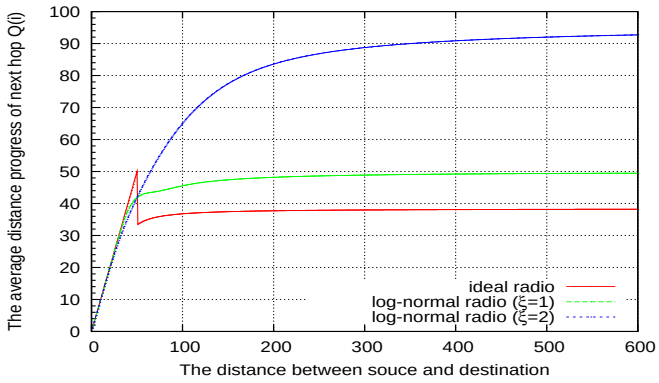

Fig. 8. average distance progress of next hop given the distance

C. Approximation of Mean Hop Count

As discussed in the previous section, the exact computation of the mean hop count can be highly complex for a communication pair with a large distance. To easy this calculation, we develop a simpler approach to estimate the mean hop count in such situations (i.e. large network). In order to achieve this, we introduce a new parameter, known as the the average progress of one hop, which measures how far the packet can progress towards the destination in one hop. Given a packet at state i, its average progress of next hop, $Q(i)$, can be computed from state transition probability $P_{i,j}$. We have,

$$Q(i) = \sum_{j \in (i,0)} (i-j) P_{i,j} \tag{33}$$

The example of average progress is illustrated in Fig. 8. It shows that $Q(i)$ increases and converges to a certain value with the distance approaching to infinite. However, the increasing rate and convergence value is different for each radio models. Let λ be the converged value for the average progress in a particular radio model. Clearly, λ is an upper bound of average progress $Q(i)$ for any i in that radio model. Let $\widetilde{H(i)}$ denote the estimated mean hop count of a communication pair separated by distance i. If we use λ to represent the average progress for each hop from distance i to the destination, we can easily estimate the mean hop count as,

$$\widetilde{H(i)} = \frac{i}{\lambda} \tag{34}$$

Since the average progress $Q(i)$ is closer to the convergence value of λ with the increase of i, we expect that this estimation can accurately approximate the actual hop count for a large i. Therefore, if we can estimate λ, we can reduce the time complexity of hop count computation to O(1) in a large network. In the rest of this section, we theoretically analyze the convergence value of λ. We first define the value of λ for ideal radio model and then extend it for log-normal shadowing radio model. In the end of this

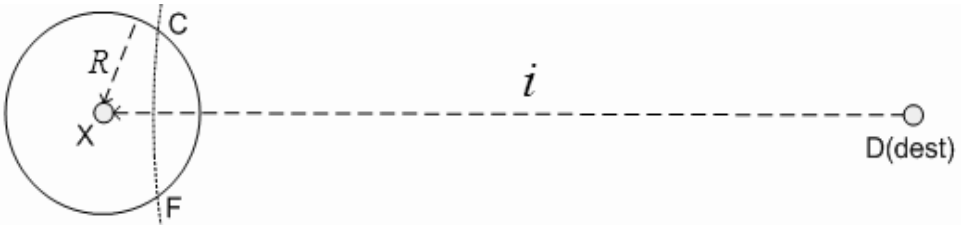

Fig. 9. As $i >> R$, the arc $\widehat{CF}$ can be approximated as line CF

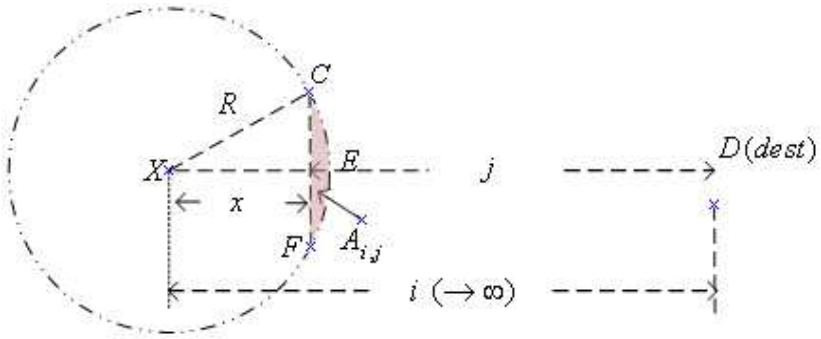

Fig. 10. As i tends to infinity, $A_{i,j}$ is approximated by the shaded region

section, we illustrate the performance of the simplified estimation by comparing the estimated results to the original analysis results of hop count.

Theorem 4: In ideal radio mode, the average progress of next hop at distance i converges as $i >> R$ and the value λ that it converges to is given by,

$$\lambda = R\Big[1 - \int_0^1 \exp(-\rho R^2(\arccos(t) - t\sqrt{1-t^2})dt)\Big] \tag{35}$$

Proof:

From Theorem 1, we know that the transition probability $P_{i,j}$ is dependent on the area of $A_{i,j}$. Fig. 2 illustrates that $A_{i,j}$ is determined by the shape of curve $\widehat{CF}$. This area is computed using Eq. (9) and depends on both i and j. If the distance i between the source and destination is very large, as depicted in Fig. 9, the curve $\widehat{CF}$ can be approximated by a straight line. Consequently, this simplifies the computation of the area $A_{i,j}$, which now solely depends on the distance between node X and its next one-hop neighbor, $i-j$. Let x represent $i-j$. Now, we can calculate the area of $A_{i,j}$, as depicted in Fig. 10, as follows,

$$A_{i,j} = 2(A_{\widehat{CXE}} - A_{CXO}) = R^2 \arccos\frac{x}{R} - x\sqrt{R^2 - x^2} \tag{36}$$

In order that the progress made along the next hop from node X towards the destination (i.e. change of state from i to j) is less than x, all neighbors of X must reside in the region to the left of CF. In other words, there is no nodes in region $A_{i,j}$. Let T represent the progress made along this hop towards the destination. The probability that the progress of the next hop towards to destination is less than x is,

$$\begin{aligned} F_T(x) &= P(T < x) \\ &= P(\text{no nodes in region } A_{i,j}) \\ &= \exp(-\rho A_{i,j}) \\ &= \exp(-\rho(R^2 \arccos \tfrac{x}{R} - x\sqrt{R^2 - x^2})) \end{aligned} \tag{37}$$

Consequently, the probability density function (pdf) of the progression T is given by,

$$f_T(x) = \frac{d}{dx} F_T(x) \tag{38}$$

Further, the average of the progression T is,

$$E(T) = \int_{-R}^{R} x f_T(x) dx \tag{39}$$

Recall that λ denotes the converged average progress. Thus, we have,

$$\begin{aligned} \lambda = \quad & E(T) = \int_0^R x f_T(x) dx \\ = \quad & \int_0^R x dF_T(x) \\ = \quad & [x F_T(x)]_{-R}^{R} - \int_0^R F_T(x) dx \\ = \quad & R - \int_0^R \exp(-\rho(R^2 \arccos \frac{x}{R} - x\sqrt{R^2 - x^2})) dx \\ \overset{x=Rt}{\Longrightarrow} \quad & R\left[1 - \int_0^1 \exp(-\rho R^2(\arccos(t) - t\sqrt{1-t^2})) dt\right] \end{aligned} \tag{40}$$

Hence theorem 4 is proved. ♠

Now we proceed to analyze the λ for log-normal shadowing radio model where the signal randomness presents. Using similar approach, we have,

Theorem 5: Under the consideration of log-normal shadowing radio model, the average progression of next hop at distance i converges as $i >> R$ and the value λ that it converges to is given by,

$$\lambda = R'\left(1 - \int_0^1 \exp(-\rho R^2(\arccos(t) - t\sqrt{1-t^2})) \cdot g(t) dt\right) \tag{41}$$

where R' satisfies $P_\wedge(R') = \alpha$ (α is a very small decimal, e.g. 0.01), and $g(t)$ is,

$$\begin{aligned} g(t) \quad = & \frac{10}{\sqrt{2\pi}\ln(10) \cdot \xi(\arccos t - t\sqrt{1-t^2})} \cdot \\ & \int_t^1 \frac{u^2 \arccos \frac{t}{u} - t\sqrt{u^2 - t^2}}{u} \exp(-(\frac{10}{\sqrt{2}\xi} log_{10} \frac{R'u}{R})^2) du \end{aligned} \tag{42}$$

Proof:

In log-normal shadowing radio model, the signal attenuation between two nodes is not only dependent on the distance separating the two nodes but also a random shadowing value. As a result, the radio range of a node is not a perfect circle. However, we can still estimate a large circle around a node, which is large enough to cover the node's all immediate one-hop neighbors with a high probability. Let R' be the radius of such large circle of a node. We first define the value of R' and then we apply the similar approach used in proofing theorem 4 to estimate λ for log-normal shadowing radio model.

Recall that the probability that there exists a direct link between two nodes separating by distance s is expressed as

$$P_{\wedge}(s) = \frac{1}{2}\left[1 - erf(\frac{10}{\sqrt{2}\xi} log_{10}\frac{s}{R})\right], \quad \xi = \sigma/\alpha \tag{43}$$

The link probability $P_{\wedge}(s)$ is a decreasing function as the distance s increases, as illustrated in Fig. 3. Given a particular distance R', if $P_{\wedge}(R')$ is very small (e.g. $\alpha = 0.01$), it means that there is rarely a direct link between two nodes if their distance is greater than R'. In other words, R' can be approximately considered as the maximum radio range of each node. According to the definition, R' can be calculated as the distance that satisfies $P_{\wedge}(s) = \alpha$, where α is a very small value.

Now we can reuse the Fig. 9 and Fig. 10 to continue the proof if we change the symbol R to R' (i.e. from the average radio range to the maximum radio range). Clearly, when $i \gg R'$, as depicted in Fig. 9, the curve $\widehat{CF}$ can be approximated by a straight line. Consequently, the area of $A_{i,j}$ depends on the relative distance of i to j (i.e. x) and becomes irrelevant to i. We have

$$A_{i,j} = 2(A_{\widehat{CXE}} - A_{CXO}) = R'^2 \arccos\frac{x}{R'} - x\sqrt{R'^2 - x^2} \tag{44}$$

In order that the progress made along the next hop from node X towards the destination (i.e. change of state from i to j) is less than x, all neighbors of X must reside in the region to the left of CF. In other words, there is no nodes in region $A_{i,j}$, or there are some nodes in region $A_{i,j}$ but all these nodes do not have direct links to node X. Let T represent the progress made along this hop towards the destination. The probability that the progression of the next hop towards to destination is less than x is,

$$\begin{aligned} F_T(x) &= P(T < x) \\ &= P(\text{no direct link from } X \text{ to all nodes in region } A_{i,j}) \\ &= \sum_{k=0}^{\infty} \Big\{ Prob(\text{k nodes in } A_{i,j}) \cdot \\ &\qquad Prob(\text{no direct link from } X \text{ to any one of those } k \text{ nodes}) \Big\} \end{aligned} \tag{45}$$

Since nodes distribution follows a Poisson point process, the number of nodes within $A_{i,j}$ have a Poisson distribution with mean $\rho A_{i,j}$. Let $g(x)$ be the probability that there is a direct link from X to a node given the node is within region $A_{i,j}$ (note that $x = i - j$). Therefore,

$$Prob(\text{k nodes in } A_{i,j}) = \frac{(\rho A_{i,j})^k}{k!} \exp(-\rho A_{i,j}) \tag{46}$$

$$Prob(\text{no direct link from } X \text{ to any one of those } k \text{ nodes}) = (1 - g(x))^k \tag{47}$$

Thus $F_T(x)$ can be rewritten as ,

$$\begin{aligned} F_T(x) &= \sum_{k=0}^{\infty} \left\{ \frac{(\rho A_{i,j})^k}{k!} \exp(-\rho A_{i,j}) \cdot (1 - g(x))^k \right\} \\ &= \exp(-\rho A_{i,j} g(x)) \sum_{k=0}^{\infty} \frac{[\rho A_{i,j}(1 - g(x))]^k}{k!} \exp[-\rho A_{i,j}(1 - g(x))] \\ &= \exp(-\rho A_{i,j} g(x)) \\ &= \exp(-\rho(R'^2 \arccos \tfrac{x}{R'} - x\sqrt{R'^2 - x^2}) \cdot g(x)) \end{aligned} \tag{48}$$

The probability density function (pdf) of the progression T is given by,

$$f_T(x) = \frac{d}{dx} F_T(x) \tag{49}$$

Therefore, the expectation of the progression T, i.e. λ, is,

$$\begin{aligned} \lambda = \quad & E(T) = \int_0^{R'} x f_T(x) dx \\ = \quad & \int_0^{R'} x dF_T(x) \\ = \quad & \Big[x F_T(x) \Big]_0^{R'} - \int_0^{R'} F_T(x) dx \\ = \quad & R' - \int_0^{R'} \exp(-\rho(R'^2 \arccos \frac{x}{R'} - x\sqrt{R'^2 - x^2}) \cdot g(x)) dx \\ \overset{x=R't}{\Longrightarrow} \quad & R' \left(1 - \int_0^1 \exp(-\rho R^2 (\arccos(t) - t\sqrt{1 - t^2})) \cdot g(t) dt \right) \end{aligned} \tag{50}$$

Now, we proceed to solve the $g(x)$, i.e, the probability that a node has a direct link to X given that the node is within the region $A_{i,j}$. Assume that node M is inside $A_{i,j}$, as shown in the Fig. 11. According to Poisson point process distribution, node M is uniformly distributed within $A_{i,j}$. Let S denote the random variable of distance between M and X. Given a particular value of s, the probability that variable S less than the value s is the probability that the node M falls within the shaded region depicted in Fig. 11. The figure shows that the shaded region has similar shape as $A_{i,j}$ but with a reduced size. Let $A_{i,i-s}$ represent the shaded region. The cumulative distribution function (cdf) of random variable S can be expressed as,

$$\begin{aligned} F_S(s) &= Prob(S < s) = \frac{\text{area of } A_{i,i-s}}{\text{area of } A_{i,j}} \\ &= \frac{s^2 \arccos \frac{x}{s} - x\sqrt{s^2 - x^2}}{R'^2 \arccos \frac{x}{R'} - x\sqrt{R'^2 - x^2}} \end{aligned} \tag{51}$$

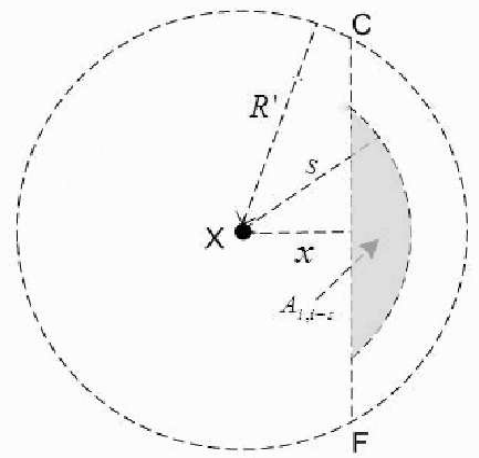

Fig. 11. Illustration used to calculate the cdf of random variable S

Consequently, the probability density function (pdf) of S is,

$$f_S(s) = \frac{d}{ds} F_S(s) \tag{52}$$

The probability that there exists a direct link between M and X is

$$\begin{aligned} g(x) &= \int_x^{R'} f_S(s) P_\wedge(s)(s) ds \\ &= \int_x^{R'} P_\wedge(s) dF_S(s) \\ &= \Big[P_\wedge(s) F_S(s) \Big]_0^{R'} - \int_x^{R'} F_S(s) dP_\wedge(s) \\ &= P_\wedge(R') + \int_x^{R'} F_S(s) \frac{10}{\sqrt{2\pi} \ln(10) \cdot \xi s} \exp(-(\frac{10}{\sqrt{2}\xi} log_{10} \frac{s}{R})^2) ds \\ &= \frac{10}{\sqrt{2\pi} \ln(10) \cdot \xi (R'^2 \arccos \frac{x}{R'} - x\sqrt{R'^2 - x^2})} \cdot \\ &\quad \int_x^{R'} \frac{s^2 \arccos \frac{x}{s} - x\sqrt{s^2 - x^2}}{s} \exp(-(\frac{10}{\sqrt{2}\xi} log_{10} \frac{s}{R})^2) ds \end{aligned} \tag{53}$$

Replace x with $R't$ and s with $R'u$, we have,

$$\begin{aligned} g(t) &= \frac{10}{\sqrt{2\pi} \ln(10) \cdot \xi (\arccos t - t\sqrt{1 - t^2})} \cdot \\ &\quad \int_t^1 \frac{u^2 \arccos \frac{t}{u} - t\sqrt{u^2 - t^2}}{u} \exp(-(\frac{10}{\sqrt{2}\xi} log_{10} \frac{R'u}{R})^2) du \end{aligned} \tag{54}$$

Finally combining Equation (50) and (54), the theorem is proved. ♠

We use Fig. 12 to illustrate the results of theorem 4 and 5, assuming $\rho = 0.0019, R = 50m$. The convergence value of λ for ideal radio model can be calculated straightforward using theorem 4. In the case of log-normal shadowing radio model (i.e. in theorem 5), we have a parameter α, which is a very

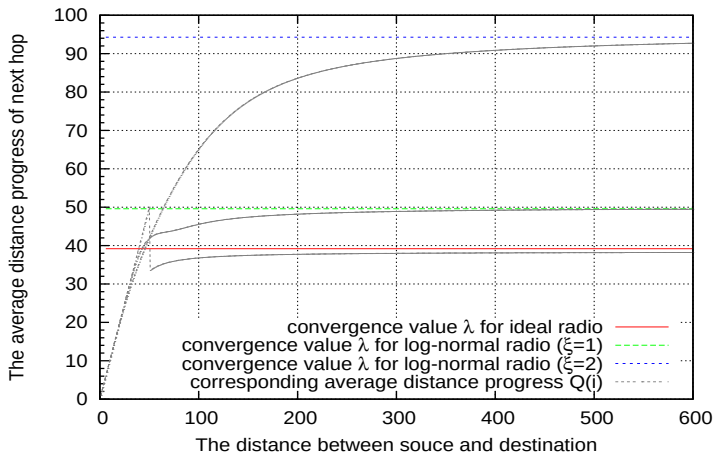

Fig. 12. Convergence value of average distance progress

small decimal and determines the approximation of nodes' maximum radio range, i.e. R'. In this example, we assume $\alpha = 1.0 \times 10^{-6}$. Correspondingly, based on the relation of $P_{\wedge}(R') = \alpha$, the R' is $150m$ and $300m$ for $\xi = 1$ and $\xi = 2$ respectively. Note that the maximum radio range R' is three times larger than the average radio range R (50m) when $\xi = 1$ and it expands to six times larger than R when ξ increases to 2. Knowing the value of R', the convergence value λ can be calculated according to theorem 5.

Fig. 12 compares the average progress of next hop to its analytical convergence value of λ under different radio model parameters. The figure clearly shows that the average progress converges to the analytical value and therefore justify Theorem. 4 and 5.

Knowing the value of λ, we can readily estimate the mean hop count of a communication pair. According to Equation. 34, we have the following corollary.

Corollary 1: Given a communication pair separated by distance i, the lower bound of its mean hop count of is

$$\widetilde{H(i)} = \frac{i}{\lambda} \tag{55}$$

where λ is the convergence value of average progress of one hop, and it is defined in Theorem 4 and 5 for ideal radio model and log-normal shadowing radio model respectively.

This estimation only needs time complexity of $O(1)$, which reduces the original complexity of analysis significantly. The comparisons of the estimation results to the original analysis results are illustrated in Fig. 13. The figure shows that the Corollary (1) can accurately approximate the mean hop count for ideal radio model and the log-normal radio model with small ξ. In the case of large value of ξ, the estimation can still serve as a lower bound of the mean hop count. Further, Fig. 13 shows that the estimations

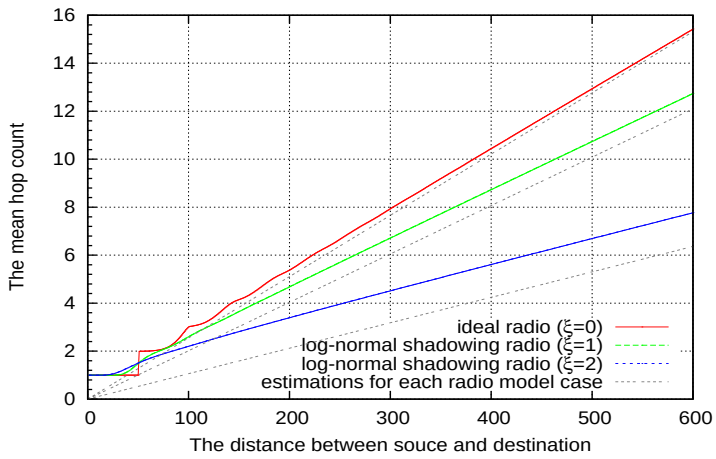

Fig. 13. The lower bound estimation of mean hopcount

becomes more accurate with the increase of the distance for all radio models. For example, in the case of $\xi = 2$, the accuracy of the estimation is 76% when $i = 400m$, while the accuracy reaches to 83% when the distance i increases to 600m. Therefore, the proposed estimation in Corollary (1) can approximate the mean hop count for a large value of i, especially when $i \gg R$.

VI. Simulation Results

In this section, we present a comprehensive set of simulations to validate our theoretical analysis. we developed a custom C++ simulator, which allows us to evaluate the results for the state transition probabilities, the hop count distribution and its mean values. In the first part of our simulations, where we validate our analysis, we use the network scenarios that conform to the assumptions made in the section III. In the second part, we relax some assumptions, e.g. the assumptions of homogenous Poisson point distribution and the network without boundary. We use the popular Random Way Point and the realistic movement traces of a vehicular network to generate two realistic network topologies. The objective of this exercise is to compare our analytical results with those from more realistic scenarios and more importantly to ascertain if the analysis can serve as bounds in these situations.

A. Scenarios Conform to the Assumptions

Recall that, our analysis assumes that the network has no boundaries. To realize this we simulate a large square network, and select a smaller square network at the center of this large network as the target network for our simulations. A similar approach is also used in [23]. We consider a square region of size $400m \cdot 400m$, and assume that nodes are deployed with a node density of $\rho = 0.0019$ (resulting

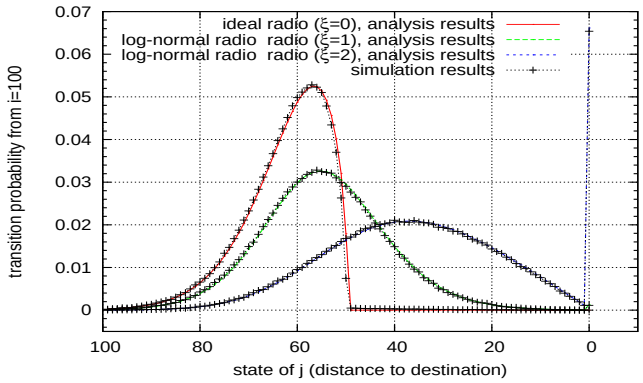

Fig. 14. State transition probability from $i = 100$ ($R = 50$)

in a total of 304 nodes averagely). The average radio range of each node, R, is assumed to be $50m$. Thus the average number of one-hop neighbors m, derived by $m = \rho\pi R^2$, is equal to 15. We simulate three values of the signal randomness parameter ξ, i.e. 0, 1, and 2, where 0 represents the ideal radio model and other values represent the log-normal shadowing radio model. For each case of ξ, we run 5000 simulations and the results presented are averaged over all runs.

For an individual run of the simulation, we randomly deploy nodes according to homogenous Poisson point process with a density of $\rho = 0.0019$. Once the nodes are placed, we use the appropriate radio model with the particular value of ξ to generate link connectivity over all pairs of nodes. Then for each pairs of nodes in the target network, we employ greedy routing to find the routing path from the one node (the source) to another (the destination). Once the routing paths are established, we can identify the next hop node for each individual node. This enables us to determine the next hop state j for each current state i. Grouping the transitions from all nodes located at distance i from the destinations gives us the distribution of the transition probabilities from state i. For each pairs, we also record its source-to-destination distance and the hop count. Then we cluster the pairs that have same source-to-destination distance together and compute the mean hop count and its distribution for each distance case.

Fig. 14 compares the simulation results of state transition probability with the corresponding analysis results derived in theorem 1 and 2. It shows that the simulations results are perfect in line with the analysis results, and therefore justifies that our model can accurately calculate the state transition probability.

Fig. 15 shows the hop count distribution comparison between the simulation results and the analysis results under ideal radio model scenario. It illustrates the hop count distribution of two communication pairs. One is with the source-to-destination distance of 100m and another is 300m. Similar, Fig. 16 and Fig. 17 illustrate the hop count distribution for log-normal radio model with randomness parameter $\xi$of 1

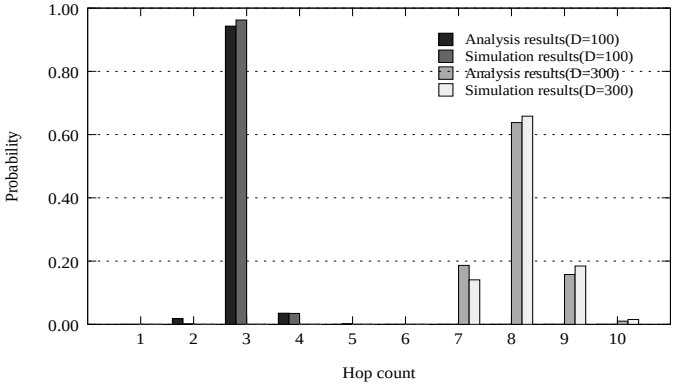

Fig. 15. Hop count distribution comparison in ideal radio model

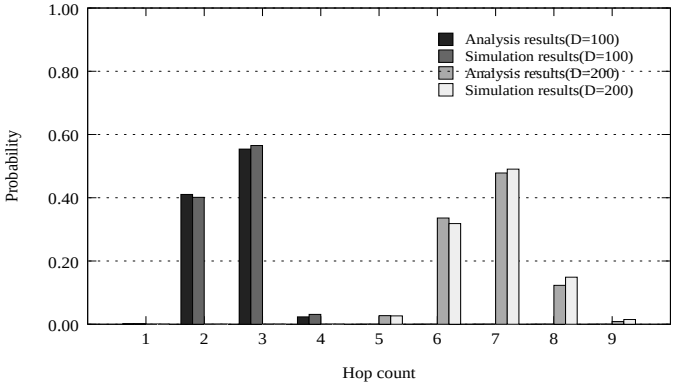

Fig. 16. Hop count distribution comparison in log-normal radio model ($\xi = 1$)

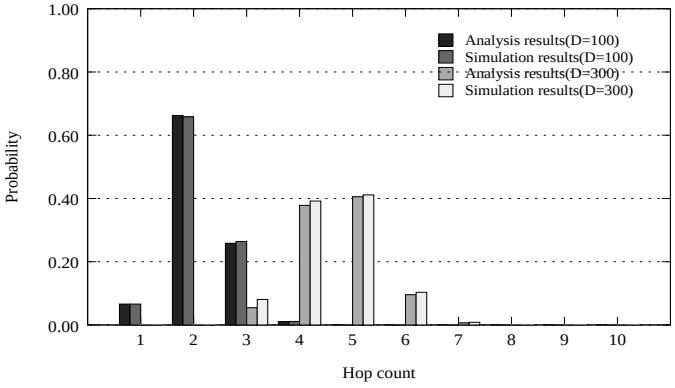

Fig. 17. Hop count distribution comparison in log-normal radio model ($\xi = 2$)

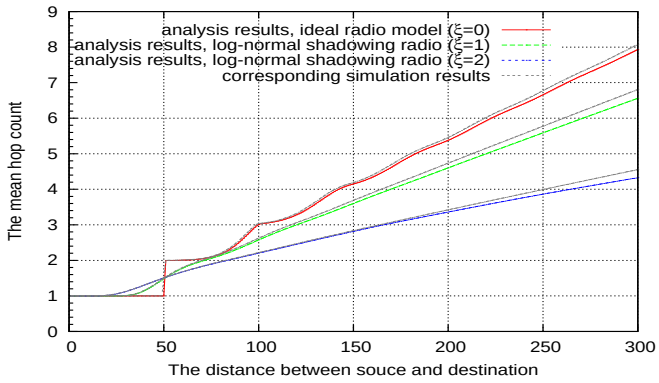

Fig. 18. Mean hop count comparison of simulation results to analysis results

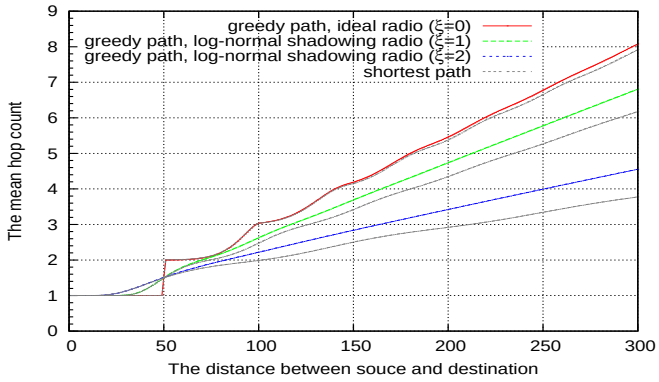

Fig. 19. mean hop count comparisons between shortest path and greedy path

and 2 respectively. The close matching between the simulation and analysis results in these three figures validates the the analytical model of hop count distribution derived in theorem 3.

Comparing the hop count distribution results, i.e. Fig. 15, Fig. 16 and Fig. 17, we can see that hop count is more evenly distributed when the signal randomness is increasing. For example, for ideal radio model (i.e. with zero signal randomness), the hop count of 8 clearly dominates the distribution of $D = 300m$ with the probability of 0.6, as shown in Fig. 15. However, when the signal randomness increases to 2, the dominating probability of $D = 300m$ drops to 0.4, and it happens at both hop count 4 and 5, shown in Fig. 17.

Fig. 18 depicts the mean hop count with varying source-to-destination distance for the different radio model. All these figures show that the simulation results are in line with our theoretical results. Thus the results validate our analysis exercise.

To understand how the routing path in greedy routing resembles the shortest routing path in term of hop count, we also simulate the hop count incurred in the shortest path routing. The comparison is illustrated

in Fig. 19. It shows that the greedy routing matches the shortest path very well in term of mean hop count when ideal radio model is used. However, in log-normal radio, the greedy routing exhibits a noticeable difference compared to the shortest path. The difference is becoming more prominent with the increasing of signal randomness ξ. These results reveal that the statement of "greedy routing can approximate find the shortest path in a relative dense network" claimed in some previous work [1], [15] only applies for ideal radio model.

B. Realistic Scenarios Not Conform to Assumptions

In the previous sub-section, all simulations parameters conformed to the assumptions used in our analysis. However, not all these assumptions will hold true for realistic wireless ad-hoc networks. In particular, a real-world network would not usually consist of homogenous Poisson point distributed nodes or uniformly distributed nodes. In this sub-section, we wish to investigate if our theoretical results are relevant in practical scenarios. For this we first use the popular random way point mobility model [29] to model a none-uniformly distributed nodes. In the second instance, we investigate a real-world vehicular ad hoc network, a popular application domain for MANETs. Our aim is to determine if the mean hop count as derived in our analysis are pertinent for these real-world networks.

For the first case we choose a scenario that uses the random way point mobility to model the nodes distribution. In random way point model, each node randomly selects a moving destination and a moving speed from the predefined speed range. The node then moves to the destination at the selected speed. After the node reaches to the destination, it pauses for a certain duration, also randomly determined, and then selects the next destination and repeat the process.

The simulated network is a square region with size of $400m \cdot 400m$. The total number of nodes is 304, which leads to the average node density of $\rho = 0.0019$. Each node has the radio range of 50 meters. The speed of each node varies uniformly from 0 to 20 m/s (i.e. from 0km/hour to 72km/hour) and the pause time is assumed to be zero.

A simulation run lasts for 5000 seconds during which we take a snapshot of the network every five seconds. For each snapshot, we use the same approaches employed in previous section to simulate the hop count results. First, we use the appropriate radio model with the particular value of ξ to generate link connectivity over all pairs of nodes. Then for each pairs, we employ greedy routing to find the routing path from the one node (the source) to another (the destination). For each pairs, we record its source-to-destination distance and the hop count. Finally we cluster the pairs that have same source-to-destination distance together over all snapshots and compute the mean hop count for each distance case.

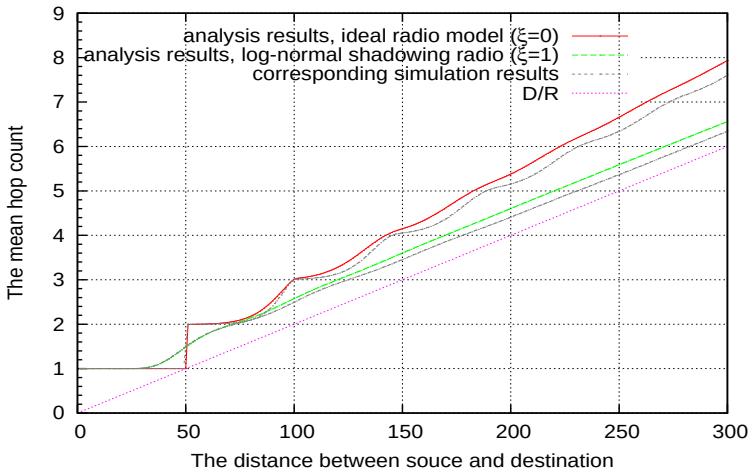

Fig. 20. mean hop count comparisons for random way point model

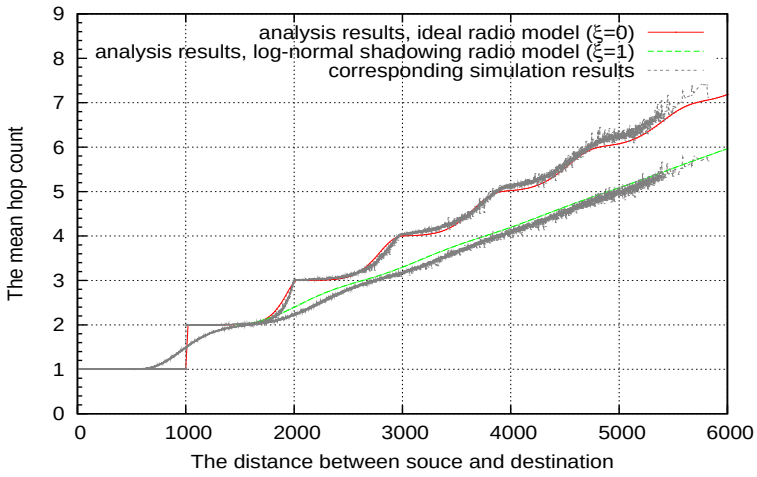

Fig. 21. mean hop count comparisons for realistic vehicular networks

Fig. 20 illustrates that our analytical results slightly over-estimate the mean hop count as compared to the simulations. The reason for this is that in the random way point model, nodes tend to move towards the central area of the network, with the consequence that the central area is much denser as compared to the regions near the border [29]. Hence, on average, the progress made per hop towards the destination is larger as compared to a purely uniform distribution (as in our analysis), resulting in a shorter hop count. However, Fig. 20 clearly demonstrates that our results are far more accurate than the frequently used measure of the mean hop count, D/R.

The mobility model used in the second instance of our simulations is based on the actual movement of buses in the King County Metro bus system in Seattle, Washington [30]. We extract an area of size

$4000m * 7000m$ corresponding to the the downtown area of Seattle. The duration of this trace spans 30 minutes. We assume that the radio range of each node is 1000m, which is consistent with that for DSRC [31] and the results from [32]. During this simulation run, we found that the average number of nodes in the selected region was 288, and thus the nodes density is $1.03 * 10^(-5)$. We apply these identical parameters to the analytical model and generate the mean hop count results. Fig. 21 compares the analysis results with those from the simulations for this realistic vehicular network. It is evident that the analysis results are well matched with those from the simulations.

VII. Conclusion

Motivated by the fundamental role of hop count in the performance analysis in multi-hop wireless ad-hoc networks, this paper proposes an accurate analytical model to estimate the hop count metric for greedy geographic routing. We formulate the hop count distribution and the mean value given a communication pair under the consideration of both ideal radio model and the realistic log-normal shadowing model. The analysis results shows that the radio model has a great impact on the hop count metric. We further propose the approximations to simplify the mean hop count analysis, which reduce the time complexity significantly. We conduct a rich set of simulations that validate the analytical model. The analysis results are further confirmed through a trace driven simulation of a practical vehicular ad-hoc network that exhibits realistic topologies of public transport buses in a metropolitan city.

The derived hop count knowledge can be incorporated in performance analysis in multi-hop wireless ad-hoc network, or assisting routing protocol design. For example, several work [33] [34] [35] have concluded that the throughput of a given communication pair is inversely proportional to the hop count from the source to the destination. Therefore, the hop count knowledge can be used as a fundamental element to estimate the throughput of wireless ad-hoc networks. Further, the hop count of a traffic flow represents the number of retransmissions of a packet experiences from the source to the destination, which can be used to determine the traffic load volume (including relay transmissions) imposed on routing layer [36]. Last but not least, we can apply the probability distribution of hop count to assist protocol design, e.g. the distance-based local geocasting protocol as discussed in [37].

References

[1] J. Li, C. Blake, D.S.J. De Couto, H.I. Lee, and R. Morris. Capacity of ad hoc wireless networks. In *Proceedings of ACM MOBICOM*, Rome, Italy, July 2001.

[2] P. Gupta and P.R. Kumar. The capacity of wireless networks. *IEEE Transactions on Information Theory*, 46(2):388–404, March 2000.

[3] G.K. Holland and N.K. Vaidya. Analysis of tcp performance over mobile ad hoc networks. *Wireless Networks*, 8(2-3):275 – 288, March 2002.

[4] J.H. Chang and L. Tassiulas. Energy conserving routing in wireless ad-hoc networks. In *Proceedings of IEEE INFOCOM*, Tel Aviv, Israel, 2000.

[5] R. Draves, J. Padhye, and B. Zill. Routing in multi-radio, multi-hop wireless mesh networks. In *Proceedings of ACM MOBICOM*, Philadelphia, PA, USA, September 2004.

[6] M. Grossglauser and DNC Tse. Mobility increases the capacity of ad hoc wireless networks. *IEEE/ACM Transactions on Networking*, 10(4):477–486, August 2002.

[7] L. Kleinrock and J. A. Silvester. Optimum transmission radii for packet radio networks or why six is a magic number. In *Proceedings of the IEEE National Telecommunications Conference*, Birmingham, Alabama, USA, December 1978.

[8] D. Lebedev and J. M. Steyaert. Path lengths in ad hoc networks. pages 207–211. 2004 international workshop on wireless ad hoc network, May 2004.

[9] S. De, A. Caruso, T. Chaira, and S. Chessa. Bounds on hop distance in greedy routing approach in wireless ad hoc networks. *International Journal on Wireless and Mobile Computing (accepted)*, 2006.

[10] L. Zhao and Q. Liang. Hop-distance estimation in wireless sensor networks with applications to resources allocation. *EURASIP Journal on Wireless Communications and Networking*, 2007.

[11] C. Bettstetter and J. Eberspacher. Hop distances in homogeneous ad hoc networks. In *Vehicular Technology Conference, 2003. VTC 2003-Spring. The 57th IEEE Semiannual*, volume 4, pages 2286–2290, April 2003.

[12] S. Dulman, M. Rossi, P. Havinga, and M. Zorzi. On the hop count statistics for randomly deployed wireless sensor networks. *International Journal of Sensor Networks*, 1:89–102, 2006.

[13] S. Mukherjee and D. Avidor. On the probability distribution of the minimal number of hops between any pair of nodes in a bounded wireless ad-hoc network subject to fading. In *Proceedings of International Workshop Wireless Ad-Hoc Networks (IWWAN)*, May 2005.

[14] Gang Zhou, Tian He, Sudha Krishnamurthy, and John A. Stankovic. Models and solutions for radio irregularity in wireless sensor networks. *ACM Transactions on Sensor Networks TOSN*, 2(2):221–262, 2006.

[15] B. Karp and H. T. Kung. GPSR: Greedy perimeter stateless routing forwireless networks. In *Proceedings of 6th Annual International Conference on Mo-bile Computing and Networking (MobiCom 2000)*, pages 243–254, Boston, MA, USA, 2000.

[16] H. Luo, F. Ye, J. Cheng, S. Lu, and L. Zhang. TTDD: Two-tier data dissemination in large-scale wireless sensor networks. *Wireless Networks*, 11:161–175, March 2005.

[17] Guoliang Xing, Chenyang Lu, Robert Pless, and Qingfeng Huang. On greedy geographic routing algorithms in sensing-covered networks. In *MobiHoc '04: Proceedings of the 5th ACM international symposium on Mobile ad hoc networking and computing*, pages 31–42, 2004.

[18] S. Basagni, I. Chlamtac, VR. Syrotiuk, and BA. Woodward. A distance routing effect algorithm for mobility (DREAM). In *Proceedings of ACM MOBICOM*, 1998.

[19] T. Camp amd J. Boleng, B. Williams, L. Wilcox, and W. Navidi. Performance comparison of two location based routing protocols for ad hoc networks. In *Proceedings of IEEE INFOCOM*, 2002.

[20] David B. Johnson, David A. Maltz, and Josh Broch. DSR: the dynamic source routing protocol for multihop wireless ad hoc networks. pages 139–172, 2001.

[21] C. E. Perkins and E. M. Royer. Ad-hoc on-demand distance vector routing (AODV). *WMCSA*, 00:90–100, 1999.

[22] S. De. On hop count and euclidean distance in greedy forwarding in wireless ad hoc networks. *IEEE Communications Letters*, 9(11), November 2005.

[23] C. Bettstetter. Connectivity of wireless multihop networks in a shadow fading environment. *Wireless Network*, 11(5):571–579, 2005.

[24] R. Hekmat and P. Van Mieghem. Connectivity in wireless ad-hoc networks with a log-normal radio model. *Mobile Networks and Applications*, 11(3):351–360, 2006.

[25] D. Miorandi and E. Altman. Coverage and connectivity of ad hoc networks presence of channel randomness. *INFOCOM 2005. 24th Annual Joint Conference of the IEEE Computer and Communications Societies. Proceedings IEEE*, 1:491–502, March 2005.

[26] C. Bettstetter and O. Krause. On border effects in modeling and simulation of wireless ad hoc networks. In *Proceedings of IEEE MWCN*, Recife, Brazil, 2001.

[27] C. Lantuejoul. *Book: Geostatistical Simulation: Models and Algorithms*. Springer, page 121, 2001.

[28] A. Baddeley, P. Gregori, J. Mateu, R. Stoica, and D. Stoyan. *Book: Case Studies in Spatial Point Process Modeling*. Springer, page 18, 2006.

[29] C. Bettstetter, H. Hartenstein, and X. Prez-Costa. Stochastic properties of the random waypoint mobility model. *Wireless Networks*, 10(5):555–567, September 2004.

[30] J. G. Jetcheva, Y. C. Hu, S. Palchaudhuri, A. K. Saha, and D. B. Johnson. Design and evaluation of a metropolitan area multitier wireless ad hoc network architecture. In *Proceedings of Fifth IEEE Workshop on Mobile Computing Systems and Applications*, 2003.

[31] Dedicated short range communications (DSRC). http://grouper.ieee.org/groups/scc32/dsrc/index.html.

[32] G. Setiwan, S. Iskander, S. S. Kanhere, Q. J. Chen, and K. C. Lan. Feasibility study of using mobile gateways for providing internet connectivity in public transportation vehiclesand. In *Proceedings of the ACM International Wireless Communications and Mobile Computing Conference (IWCMC)*, Vancouver, Canada, 2006.

[33] Gavin Holland and Nitin Vaidya. Analysis of tcp performance over mobile ad hoc networks. *Wireless Networks*, 8(2):275–288, 2005.

[34] C.-K. Toh, M. Delwar, and D. Allen. Evaluating the communication performance of an ad hoc wirelessnetwork. *IEEE Transactions on Wireless Communications*, 1(3):402–414, July 2002.

[35] S. Bansal, R. Gupta, R. Shorey, I. Ali, A. Razdan, and A. Misra. Energy efficiency and throughput for TCP traffic in multi-hop wireless networks. In *INFOCOM 2002. Twenty-First Annual Joint Conference of the IEEE Computer and Communications Societies. Proceedings. IEEE*, volume 1, pages 210–219, 2002.

[36] Q. Chen, S. S. Salil, and M. Hassan. Analysis of per-node traffic load in multihop wireless sensor networks. *Accepted by IEEE Transaction on Wireless Communication*, 2008.

[37] Q. Chen, S. S. Salil, M. Hassan, and Y. K. Rana. Distance-based local geocasting in multi-hop wireless networks. In *IEEE Wireless Communications and Networking Conference WCNC 2007*, March 2007.